Chinese Chemical Letters 31 (2020) 2752–2756

Contents lists available at ScienceDirect

Chinese Chemical Letters

journal homepage: www.elsevier.com/locate/cclet

Communication

Electrochemical performance of a three-layer electrode based on Bi nanoparticles, multi-walled carbon nanotube composites for simultaneous Hg(II) and Cu(II) detection

Qiwen Bao[a,1], Gang Li[a,1], Zhengchun Yang[b], Peng Pan[b], Jun Liu[b], Jiayuan Chang[b], Jun Wei[b,c], Ling Lin[a,*]

[a] School of Precision Instrument and Optoelectronic Engineering, the State Key Laboratory of Precision Measuring Technology and Instruments, Tianjin University Tianjin 300072, China
[b] School of Electrical and Electronic Engineering, Tianjin Key Laboratory of Film Electronic & Communication Devices, Advanced Materials and Printed Electronics Center, Tianjin University of Technology, Tianjin 300384, China
[c] Agency for Science, Technology and Research (A*STAR), Singapore Institute of Manufacturing Technology, Singapore 638075, Singapore

ARTICLE INFO

Article history:
Received 5 April 2020
Received in revised form 23 May 2020
Accepted 11 June 2020
Available online 18 June 2020

Keywords:
Bismuth nanoparticle
Multi-walled carbon nanotube
Electrochemical sensor
Hg(II)
Cu(II)

ABSTRACT

Electrochemical analysis is a promising technique for detecting biotoxic and non-biodegradable heavy metals. This article proposes a novel composite electrode based on a polyaniline (PANi) framework doped with bismuth nanoparticle@graphene oxide multi-walled carbon nanotubes (Bi NPs@GO-MWCNTs) for the simultaneous detection of multiple heavy metal ions. Composite electrodes are prepared on screen-printed electrodes (SPCEs) using an efficient dispensing technique. We used a SM200SX-3A dispenser to load a laboratory-specific ink with optimized viscosity and adhesion to draw a pattern on the work area. The SPCE was used as substrate to facilitate cost-effective and more convenient real-time detection technology. Electrochemical techniques, such as cyclic voltammetry and differential pulse voltammetry, were used to demonstrate the sensing capabilities of the proposed sensor. The sensitivity, limit of detection, and linear range of the PANi-Bi NPs@GO-MWCNT electrode are 2.57×10^2 μA L μmol^{-1} cm^{-2}, 0.01 nmol/L, and 0.01 nmol/L–5 mmol/L and 0.15×10^{-1} μA L μmol^{-1} cm^{-2}, 0.5 nmol/L, and 0.5 nmol/L–5 mmol/L for mercury ion (Hg(II)) and copper ion (Cu(II)) detection, respectively. In addition, the electrode exhibits a good selectivity and repeatability for Hg(II) and Cu(II) sensing when tested in a complex heavy metal ion solution. The constructed electrode system exhibits a detection performance superior to similar methods and also increases the types of heavy metal ions that can be detected. Therefore, the proposed device can be used as an efficient sensor for the detection of multiple heavy metal ions in complex environments.

Heavy metal ions such as Hg(II) and Cu(II) cause great harm to the environment and human body because of their biotoxicity and non-degradability, this renders it difficult to remove them from the food chain [1]. These heavy metal ions harm organisms in various ways. Their combinations with active groups in the structures of various enzymes in an organism can inhibit biological enzyme activities and cause bodily malfunction [2] and certain heavy metal ions cause enzyme deactivation by replacing important metal ions in the enzyme structure [3]. Mercury ions are highly toxic to the environment and the human body. Investigations indicated that 0.05 mg/L of mercury in urine can cause mercury poisoning. Mercury poisoning mainly produces symptoms such as mental disorders caused by central nervous disorders, language disorders, dyskinesias, and muscle atrophy [4]. Excess copper metal ions that enter the body mainly cause kidney and liver dysfunction and failure [5].

The following traditional methods are used for the detection of heavy metal ions: atomic absorption spectroscopy (AAS) [6], inductively coupled plasma mass spectrometry (ICP-MS) [7], ultraviolet-visible spectrophotometry (UV–vis) [8], and surface enhanced Raman spectroscopy (SERS) [9]. In recent years, the electrochemical analysis method has attracted much attention due to the simple process, low cost, low sample preparation requirements, rapid analysis, and easy miniaturization and integration for heavy metal ion detection [10].

* Corresponding author.
E-mail address: linling@tju.edu.cn (L. Lin).
[1] These authors contributed equally to this work.

https://doi.org/10.1016/j.cclet.2020.06.021

Nanoparticles (NPs) are considered promising electrode materials because they are environmentally friendly, exhibit good electrical characteristics, and involve simple synthesis steps [11]. Guo reported a one-pot hot-bath method based on the use of Bi-doped SnO_2/reduced graphene oxide (rGO) NPs for the detection of benzene gas. Its sensing performance was significantly higher than that obtained with pure SnO_2 and rGO/SnO_2 [12]. Rao studied the effect of Bi nanoions doped on p-ZnTe/n-CdS thin-film photoelectric sensors. The results indicated that the I–V and C–V characteristics of the device were significantly improved [13]. Various studies have shown that Bi NPs are usually used as dopants or compounded with other functional materials in the fields of optical and electrochemical detection owing to their excellent properties such as eco-friendliness, low cost, and ease of synthesis [14]. In this study, we employed the lower production of Bi NPs proposed by Nithiya to improve the composite film synthesis method [15]. This study involved the assembly of Bi NPs in certain functional materials or macromolecules to interact with test substances [16]. Polyaniline (PANi) materials have attracted the widespread attention of researchers because they are environmentally friendly, are easily accessible, and exhibit good redox properties and electrical conductivities. Methods for their synthesis have been studied by an increasing number of researchers [17].

Multi-walled carbon nanotubes (MWCNTs) and graphene oxide (GO) are functional materials with excellent performances and have similar physical and chemical properties such as a large specific surface area, good hydrophilicity, and excellent conductivity [18]. They also present their own unique features and disadvantages. GO is well known for the low manufacturing cost, good amphiphilicity, and good biocompatibility, but its insulation properties are poor because it contains carboxyl, hydroxyl, and epoxy groups [19]. The MWCNTs are often used as dopants because of their excellent properties such as a good chemical stability, strong catalytic ability, and excellent antifouling performance of electron transport properties [20]. However, although agglomerates may be easily formed, the formation of thin films is difficult due to strong van der Waals forces in organic solvents or deionized water [21]. Researchers reported that MWCNTs and GO flakes dissolve better in polar solutions based on π-π interactions. Doped metal NPs are generally used to improve the electrocatalytic performance of composite films. Constructed MWCNTs used as sensing materials exhibit a good repeatability, reversibility, and stability [18].

In this study, a high-performance functional area was constructed; a scaffold-like polyaniline frame was used to fix the composite structure consisting of MWCNTs and GO sheets. The MWCNTs act similar to high-speed electronic motion bridges in a three-dimensional (3D) structure and the Bi NPs are randomly scattered in the 3D scaffold.

A simple hybrid method was used in this study to dope PANi molecular chains with Bi NPs to synthesize functional materials. Subsequently, chitosan (CS)/PANi-Bi nanoparticle@graphene oxide multi-walled carbon nanotube (NPs@GO-MWCNT) screen-printed electrodes (SPCEs) were fabricated as three-layered composite electrodes for copper and mercury ion detection. We designed an electrochemical sensor based on PANi-Bi NPs@GO-MWCNTs for the detection of various heavy metal ions using a dispensing process determined by factors such as the manufacturing cost, biocompatibility, synthetic steps, and environmental concerns. A CS protective film with low biological toxicity was employed instead of a traditional ion protective film and the electrode substrate was composed of a flexible SPCE. We evaluated the selectivity and stability of the proposed sensor for the use in complex heavy metal ion environments.

As shown in Scheme 1, in Step 1, the polyethylene glycol terephthalate (PET) substrate was washed with water and ethanol and then dried. All screen-printing experiments were performed on an automatic flat screen-printing machine (WY-4060, Langfang Screen Printing Fest Screen Printing Materials Co., Ltd., China). Carbon ink with a good fluidity was printed on the PET substrate and used as conductive layer. Subsequently, it was dried for 1 h at 110 °C.

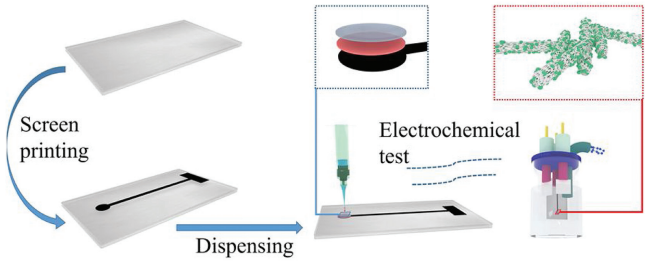

Scheme 1. Fabrication of the proposed CS/PANi-Bi NPs@GO-MWCNTs for electrocatalytic mercury and copper ion sensors.

The thickener used for the ink was prepared by mixing polyvinyl alcohol (PVA) with 4 and 96 wt% deionized (DI) water and then heated in a round-bottom beaker at 120 °C for 1 h under uniform stirring. The CS protective film solution was prepared using the following steps: 0.31 g CS was dissolved in 30 mL of 2% solution (0.6 mL pure glacial acetic acid added to 29.4 mL DI water) and stirred for 2 h to form a 1% CS protective film solution. The preparation process for the No. 1 electrode is shown in Scheme 1. First, the prepared PANi-Bi NPs@GO-MWCNTs powder and thickener were mixed at a filling ratio of 20%. A dispenser (SM200SX-3A, MUSASHI, Japan) was then used to draw a circular pattern with 1 mL of the composite material on the electrode surface at a power of ~15.9 kW. Another needle tube and needle were then used to draw 1 mL CS to paint an ion protection layer on the electrode at a power of ~9.8 kW.

Figs. S1a and b (Supporting information) show the scanning electron microscopy (SEM) images of Bi NPs@GO-MWCNTs obtained at 10 K and 200 K magnifications, respectively. The diameter of the MWCNTs was determined to be ~43.5 nm using particle size analysis. The SEM images also indicate that the MWCNTs are randomly arranged around the GO sheet and form bridges similar to those connecting the graphene sheets with the GO sheets.

Figs. S1c and d (Supporting information) show the energy-dispersive X-ray (EDX) spectroscopy data for the Bi NPs@GO-MWCNTs. Analyses of the mapping data and energy spectrum statistics indicate that Bi exists in the composite structures of the MWCNTs and GO sheets. The atomic percentages of C, O and Bi were 85.15%, 9.16%, and 4.89%, respectively. The transmission electron microscopy (TEM) (Fig. S2 in Supporting information) and EDX (inset figure) images of Bi NPs@GO-MWCNTs showed that the Bi NPs are distributed on the walls of the MWCNTs.

The X-ray diffraction (XRD) tests were performed on powders of PANi, Bi NPs@GO-MWCNTs, and PANi-Bi NPs@GO-MWCNTs composite materials in the range of 20°–70° to verify the composition of the prepared samples. The black curve in Fig. S3a (Supporting information) shows that the XRD spectrum of PANi contains three characteristic diffraction peaks at 21.36°, 23.44° and 26.86°, which are related to the (010), (100) and (110) planes of PANi. The three characteristic diffraction peaks shown in the red pattern in Fig. S3a at 25.62°, 49.5° and 54.94° correspond to the reflections of the MWCNT (002) plane [22] and the (202) and (024) planes of Bi, respectively [23]. The light blue spectrum in Fig. S3a indicates that the composite is in a co-doped state of PANi and Bi NPs@GO-MWCNTs [24].

Raman spectroscopy is often used to analyze the bonding structure of materials. As shown in Fig. S3b, the three characteristic peaks at 1345 cm^{-1}, 1574 cm^{-1}, and 2687 cm^{-1} in the Raman spectrum (red curve) of the Bi NPs@GO-MWCNTs correspond to the typical D, G, and 2D bands of MWCNTs. The characteristic peaks at 1128 cm^{-1}, 1513 cm^{-1}, and 2625 cm^{-1} with a slight left shift in the map of the PANi-Bi NPs@GO-MWCNTs composite (light green curve) indicate that the two components are uniformly distributed in the composite.

Fig. 1a shows DPVs of CS/PANi-Bi NPs@GO-MWCNTs/SPCE in 0.01 mol/L PBS for different concentrations of Hg(II). Figs. 1b and c show the linear fitting curves for the current density (A/cm^2) and the concentration (nmol/L) curve at +0.16 V in the high-concentration (0.5 − 5 nmol/L) and low-concentration (0.01 − 0.1 nmol/L) Hg(II) solutions, respectively. The CS/PANi-Bi NPs@GO-MWCNTs/SPCE shows a good linearity (R^2 = 0.87, 0.94), good average sensitivity (2.57×10^2 μA L $μmol^{-1}$ cm^{-2}) in the concentration range 0.01–5 mmol/L, and lower limit of detection (LOD < 0.02 nmol/L), which is well below the maximum contamination level for mercury in drinking water set by the United States Environmental Protection Agency [25].

A comparison of the Hg(II) detection performance of CS/PANi-Bi NPs@GO-MWCNTs/SPCE with those of various reported modified electrodes is shown in Table S1 (Supporting information). The results indicate that CS/PANi-Bi NPs@GO-MWCNTs/SPCE exhibits properties superior to those of the other materials used for Hg(II) detection, which may be related to the double-layer "scaffolding" structure used for Bi NP attachment in this study.

The cyclic voltammetry (CV) curves obtained for CS/PANi-Bi NPs@GO-MWCNTs/SPCE in the presence of 0.01–2 nmol/L and 2 μmol/L–5 mmol/L in PBS (0.01 mol/L, pH 7.2) as the supporting electrolyte are shown in Figs. S4a and b (Supporting information). The applied potential range was −0.2 V to +0.4 V. The CV curves of the solution containing 0.01–5 mmol/L Hg(II) were split into two plots to determine the oxidation and reduction peaks. The results show that anodic oxidation and cathodic reduction peaks appeared at +0.2 V and 0 V, respectively. Based on the principle of electrochemical interface reactions, the interface reaction of O_2/H_2O was ignored because N_2 is continuously transported into the electrolytic cell during the entire experiment. The oxidation and reduction reactions correspond to Cl^-/AgCl/Ag and Bi/Hg(II) interfacial reactions. The prepared CS/PANi-Bi NPs@GO-MWCNTs/SPCE three-layer composite electrode shows good electrochemical and sensing characteristics across a wide concentration range of 0.01–5 mmol/L. These results can be explained as follows: (1) The synergistic effect greatly improves the sensing performance when co-doped composites of GO, MWCNTs, and Bi NPs are used for Hg(II) detection; (2) SEM and TEM data confirm that the PANi-Bi NPs@GO-MWCNT composite material has a wide specific 3D surface area, which provides more active sites for electrocatalytic reactions; and (3) in this device, the diffusion reaction has a greater impact on the electrochemical reactions and N_2 is continuously introduced below the liquid surface, which eliminates excess interfacial reactions. The resulting bubbles also contribute to the diffusion reaction.

A heavy metal ion detector requires a sensor that functions within the acceptable parameters in complex environments (including those potentially containing many other heavy metal ions). The specificity of CS/PANi-Bi NPs@GO-MWCNTs/SPCE for Hg(II) detection was tested in PBS containing 10 μmol/L Cu(II), Fe(III), Cd(II), Cr(III), Ni(III), Pb(II), Zn(II), and 10–20 μmol/L Hg(II), as shown in Fig. 2a. The repeatability of the device was tested using a repetitive experiment (10 times) on 10 μmol/L Hg(II) in a complex solution containing the heavy metal ions mentioned above, as shown in Fig. 2b. The statistical graph of the current density (A/cm^2) is plotted *versus* the potential (V) of Fig. 2b at +0.148 V in Fig. 2c. The results indicate that CS/PANi-Bi NPs@GO-MWCNTs/SPCE maintains good specificity and stability in terms of Hg(II) detection and the performance is reduced by only 26.82%, even in complex solutions.

The characteristic peaks that appear at specific voltages compared with the control experiment (the blue curve in Fig. 2a) in Fig. 2a suggest that CS/PANi-Bi NPs@GO-MWCNTs/SPCE may have the required electrochemical properties for Cu(II) and Cd(II) detection. Differential pulse voltammetry (DPV) curves of the prepared electrode for 0.5 nmol/L–5 mmol/L Cu(II) in the voltage window of −0.4 V to +0.2 V are shown in Fig. 3a. A peak with increasing intensity can be observed, which slightly shifts to the right with increasing Cu(II) concentration in the range −0.2 V to −0.12 V. The linear fitting curve for the data in Fig. 3a is displayed in Fig. 3b, which proves the high linearity (R^2 = 0.97), increased sensitivity (0.15×10^{-1} μA L $μmol^{-1}$ cm^{-2}), and LOD (0.5 nmol/L) of the proposed electrode. A comparison of the proposed electrode with various recently reported sensors is displayed in Table 1. The results show that CS/PANi-Bi NPs@GO-MWCNTs/SPCE obtained using a simple synthesis process had excellent performance and could be used as a Cu(II) sensing electrode.

The CV data for CS/PANi-Bi NPs@GO-MWCNTs/SPCE in PBS solution containing 0.01 nmol/L–5 mmol/L Cu(II) are displayed in Fig. S5a (Supporting information). The electrodes that were modified using PANi-Bi NPs@GO-MWCNTs showed anodic oxidation and cathodic reduction peaks at +0.11 V and −0.05 V, respectively. The selectivity data for the proposed sensor is shown in Fig. S5b (Supporting information).

The DPV signal changes of the fabricated sensors were sequentially recorded in the presence of various concentrations of other metal ions (10 μmol/L) and 10 μmol/L Cu(II). The current density in the presence of Cu(II) is significantly higher than that observed in the other experiments. It is 155.2% higher than that of the

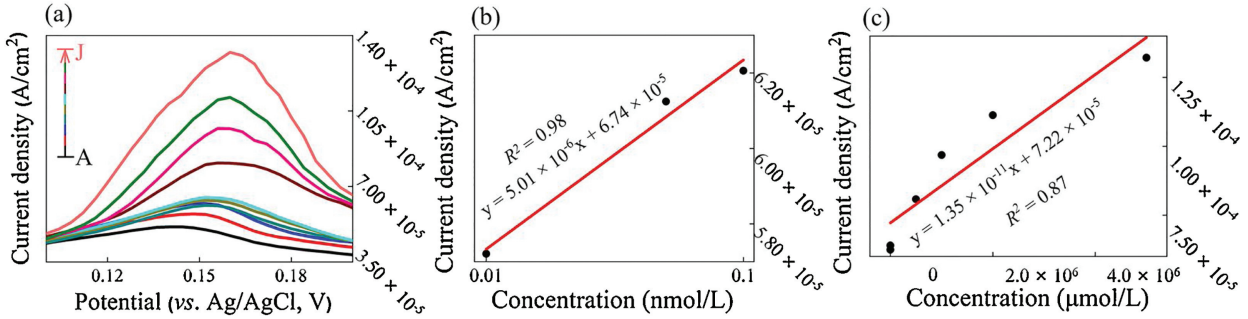

Fig. 1. (a) DPVs of CS/PANi-Bi NPs@GO-MWCNTs/SPCE in 0.01 mol/L PBS for different concentrations of Hg(II) (curves A–J: 0.02 nmol/L–5 mmol/L). (b, c) Linear calibration plot of the current density (A/cm^2) for high/low concentrations of Hg(II) (in nmol/L).

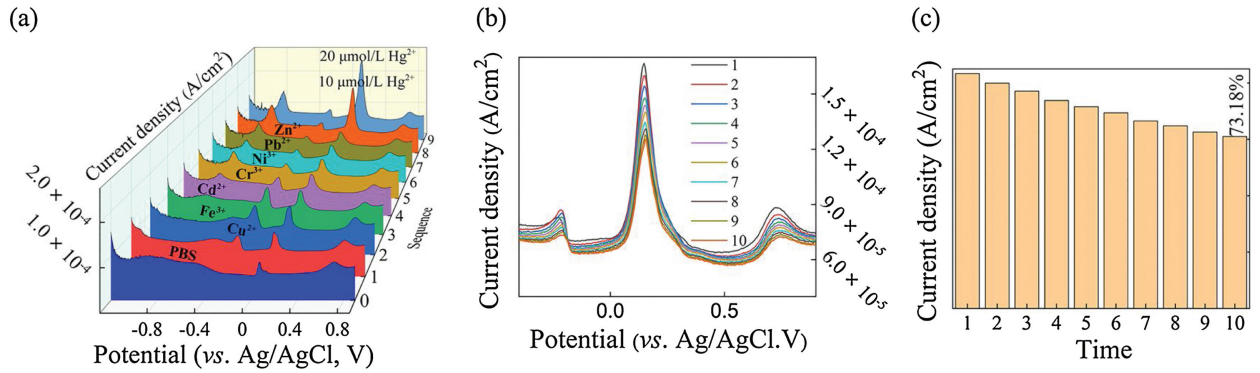

Fig. 2. (a) DPV curves obtained for Bi NPs@GO-MWCNTs/SPCE in the presence of 10 μmol/L of Cu(II), Fe(III), Cd(II), Cr(III), Ni(III), Pb(II), Zn(II) and 10–20 μmol/L Hg(II) ions in PBS (0.01 mol/L, pH 7.2). (b, c) Ten repeated tests for 10 μmol/L Hg(II) in a mixed heavy metal ion environment.

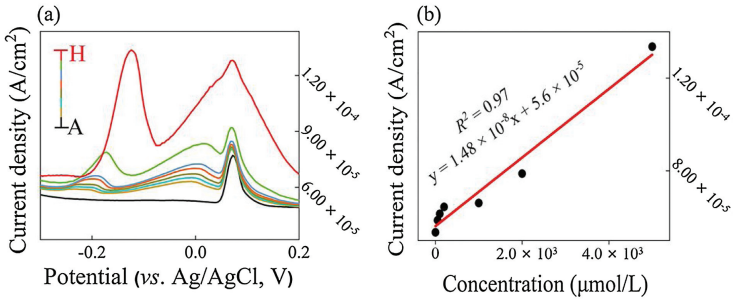

Fig. 3. (a) DPV curves obtained for Bi NPs@GO-MWCNTs/SPCE in the presence of different concentrations of Cu(II) (A-H: 0.5 nmol/L–5 mmol/L) in PBS (0.01 mol/L, pH 7.2); (b) Linear calibration plot of the current density (A/cm^2) *vs.* the Cu(II) concentration (μmol/L).

Table 1
Comparison of the analytical parameters obtained using CS/Bi NPs@GO-MWCNTs/SPCE for Cu(II) sensing with those of previous reports.

Electrode	LOD (nmol/L)	Liner range (nmol/L)	Electrode synthesis method	Ref.
PPy nanowire/PA	52.403	157.37–944.2	Electrostatic adsorption and ultrasonic mixing	[26]
PPy nanotubes	46	0.1–3 × 10^4	Electrochemicalpolymerization	[27]
HxTiS2Nanosheet-PANI/GCE	0.7	25–5000	Lithium intercalation and exfoliation method, the surface polymerization reactions of aniline	[28]
EDTA-PANI/SWCNTs	80	2000–1.2 × 10^6	Electrochemical synthesis	[29]
PANI-MC	6	10–1000	Dispersion methods	[30]
EDTA-PTh modified electrode	0.5	0.5–100	Polymerization methods	[31]
MWCNT-NS	>10,000	1000–1 × 10^8	Mixing method	[32]
CS/PANi-Bi PANi-NPs@GO-MWCNTs/SPCE	0.01	0.01–5 × 10^6	Gumming and printing methods	This work

experiments conducted in PBS. These results imply that CS/PANi-Bi NPs@GO-MWCNTs/SPCE exhibits less interference and a stronger electrochemical response to Cu(II) in the presence of other heavy metal ions. In this study, experiments were only performed on several common heavy metal ions. The potential electrochemical performance of the synthesized composite electrode with respect to other heavy metal ions has not been verified.

In this study, a modified bismuth-based NP material was prepared using a simple solvothermal method for use as an anode material in electrochemical testing. The sensors fabricated for simultaneous Hg(II) and Cu(II) detection using CS/PANi-Bi NPs@GO-MWCNTs/SPCEs demonstrate lower LODs (Hg(II): 0.01 nmol/L, Cu(II): 0.5 nmol/L), wider linear ranges (Hg(II): 0.01 nmol/L–5 mmol/L and Cu(II): 0.5 nmol/L–5 mmol/L), and higher sensitivities (Hg(II): 2.57 × 10^2 μA L μmol^{-1} cm^{-2}, Cu(II): 1.48 × 10^{-2} μA L μmol^{-1} cm^{-2}) than other currently available devices. The promising electrochemical behavior of the proposed sensor in terms of heavy metal ion detection is due to its special double-layer "scaffolding" structure that was used for the attachment of Bi NP active materials. The prepared composite electrode provides good anti-interference and stability when used for heavy metal ion detection. It could potentially be applied to detached electrodes used in portable heavy metal ion detection equipment because of the easy implementation and inexpensive processes. Research regarding portable devices for the detection of heavy metal ions in sewage is very meaningful. In the future, we will focus on the design of an inexpensive multi-channel heavy metal ion sensor device equipped with the electrode introduced in this article.

Declaration of competing interest

The authors declare that they have no known competing financial interests or personal relationships that could have appeared to influence the work reported in this paper.

Acknowledgments

The authors would like to thank the Tianjin Natural Science Foundation (Nos. 18JCZDJC99800, 7JCQNJC00900), National Natural Science Foundation of China (No. 51502203), Tianjin Young Overseas High-level Talent Plans (No. 01001502), Tianjin Science and Technology Foundation (No. 17ZXZNGX00090), Tianjin Distinguished Professor Foundation of Young Researchers, and Tianjin Development Program for Innovation and Entrepreneurship. The authors also thank the State Key Laboratory of Precision Measuring Technology and Instruments for the use of their equipment. The authors would like to thank Profs. Yang and Pan of the Tianjin University of Technology for their guidance with respect to the experimental ideas and techniques.

Appendix A. Supplementary data

Supplementary material related to this article can be found, in the online version, at doi:https://doi.org/10.1016/j.cclet.2020.06.021.

References

[1] T. Kokab, A. Shah, F.J. Iftikhar, et al., ACS Omega 4 (2019) 22057–22068.
[2] X. Dai, O. Nekrassova, M.E. Hyde, R.G. Compton, Anal. Chem. 76 (2004) 5924–5929.
[3] P.B. Tchounwou, W.K. Ayensu, N. Ninashvili, D. Sutton, Environ. Toxicol. 18 (2003) 149–175.
[4] H.N. Kim, W.X. Ren, J.S. Kim, J. Yoon, Chem. Soc. Rev. 41 (2012) 3210–3244.
[5] R. Chandra, A. Ghorai, G.K. Patra, Sens. Actuat. B-Chem. 255 (2018) 701–711.
[6] A. Jaiswal, S.S. Ghsoh, A. Chattopadhyay, Langmuir 28 (2012) 15687–15696.
[7] W. Gao, H.Y.Y. Nyein, Z. Shahpar, et al., ACS Sens. 1 (2016) 866–874.
[8] M.H. Lee, J.S. Wu, J.W. Lee, J.H. Jung, J.S. Kim, Organ. Lett. 9 (2007) 2501–2504.
[9] P. Makam, R. Shilpa, A.E. Kandjani, et al., Biosens.Bioelectron. 100 (2018) 556–564.
[10] B. Bansod, T. Kumar, R. Thakur, S. Rana, I. Singh, Biosens. Bioelectron. 94 (2017) 443–455.
[11] L. Li, D.K. Ma, F. Qi, W. Chen, S. Huang, Electrochem. Acta 298 (2019) 580–586.
[12] W.W. Guo, Q.L. Zhou, J. Zhang, et al., Sens. Actuat. B: Chem. 299 (2019) 126959.
[13] G.K. Rao, V.K. Ashith, K. Priya, P. Kumar, Sens. Actuat.-Phys. 284 (2018) 194–200.
[14] A.L. Brown, P.C. Naha, V. Benavides-Montes, et al., Chem. Mater. 26 (2014) 2266–2274.
[15] S.Y. Lim, W. Shen, Z.Q. Gao, Chem. Soc. Rev. 44 (2015) 362–381.
[16] L. Shi, Y.Y. Li, X.J. Rong, Y. Wang, S.M. Ding, Anal. Chem. Acta 968 (2017) 21–29.
[17] Q.W. Bao, Z.C. Yang, Y.F. Song, M.Y. Fan, P. Pan, J. Mater. Sci.-Mater. Electron. 30 (2019) 1751–1759.
[18] S. Tursynbolat, Y. Bakytkarim, J.Z. Huang, L.S. Wang, J. Pharm. Anal. 9 (2019) 358–366.
[19] X. Qiu, L. Lu, J. Leng, et al., Food Chem. 190 (2016) 889–895.
[20] A. Dehdashti, A. Babaei, Electroanalysis 32 (2020) 1017–1024.
[21] K.C. Ho, Y.H. Teow, A.W. Mohammad, W.L. Ang, P.H. Lee, J. Membr. Sci. 552 (2018) 189–201.
[22] Z.Y. Wang, C. Zhao, T.Y. Han, et al., Sens. Actuat. B-Chem. 242 (2017) 269–279.
[23] G.J. Lee, H.M. Lee, C.K. Rhee, Electrochem. commun. 9 (2007) 2514–2518.
[24] X.F. Lu, H. Mao, D.M. Chao, W.J. Zhang, Y. Wei, Macromol. Chem. Phys. 207 (2006) 2142–2152.
[25] D.H. Wu, Q. Zhang, X. Chu, R.Q. Yu, Biosens. Bioelectron. 25 (2010) 1025–1031.
[26] N. Wang, H.X. Dai, D.L. Wang, H.Y. Ma, M. Lin, Mater. Sci. Eng. C-Mater. Biol. Appl. 76 (2017) 139–143.
[27] M. Lin, X.K. Hu, Z.H. Ma, L.X. Chen, Anal. Chim. Acta 746 (2012) 63–69.
[28] X.R. Gan, H.M. Zhao, S. Chen, H.T. Yu, X. Quan, Anal. Chem. 87 (2015) 5605–5613.
[29] M.A. Deshmukh, R. Celiesiute, A. Ramanaviciene, et al., Electrochem. Acta 259 (2018) 930–938.
[30] Z. Guo, S. Li, X.M. Liu, et al., Mater. Chem. Phys. 128 (2011) 238–242.
[31] A. Rahman, M.S. Won, Y.B. Shim, Anal. Chem. 75 (2003) 1123–1129.
[32] M.R. Ganjali, S. Aghabalazadeh, M. Khoobi, et al., Int. J. Electrochem. Sci. 6 (2011) 52–62.